The paper was published in the proceedings of the 20th International Conference on Soil Mechanics and Geotechnical Engineering and was edited by Mizanur Rahman and Mark Jaksa. The conference was held from May 1st to May 5th 2022 in Sydney, Australia.

Proceedings of the 20th International Conference on Soil Mechanics and Geotechnical Engineering– Rahman and Jaksa (Eds)
© 2022 Australian Geomechanics Society, Sydney, Australia, ISBN 978-0-9946261-4-1

Evaluation of coefficients of restitution for rockfall modeling

Évaluation des coefficients de restitution pour la modélisation des chutes de blocs

Jean Benoît, Bruma Souza, Hannah Miller & Noah MacAdam
Department of Civil and Environmental Engineering, University of New Hampshire, USA, jean.benoit@unh.edu

ABSTRACT: Landslide hazard research at the University of New Hampshire (USA) over the last decade has led to the development of Smart Rock (SR) sensors, which have been used to instrument rockfall experiments. The latest SRs are instrumented capsules 50.8 mm in length and 25.4 mm in diameter that record data from the perspective of the falling rock. Each SR is equipped with a ±400 g and a ±16 g 3-axis accelerometer, a ±4000 dps high-rate gyroscope, and an altimeter. This paper summarizes the results of instrumented laboratory experiments to determine coefficients of restitution of sand and rock. The characteristics of the test blocks show that the energy restitution can significantly vary for different block shapes and impact surfaces. This parametric study aimed to develop a preliminary methodology to evaluate and enhance input parameters in computer rockfall modeling and help with mitigation methods. Trajectories obtained from the rockfall field experiments were also compared to 2D rockfall models to evaluate the coefficients obtained experimentally.

RÉSUMÉ : La recherche sur les risques de glissements de terrain à l'Université du New Hampshire (États-Unis) au cours de la dernière décennie a conduit au développement de capteurs Smart Rock (SR), qui ont été utilisés pour instrumenter des expériences de chute de blocs. Les derniers SR sont des capsules instrumentées de 50,8 mm de longueur et 25,4 mm de diamètre misent à l'intérieur de la roche et qui enregistrent les données lors d'une chute de bloc. Chaque SR est équipé d'un accéléromètre 3 axes ± 400 g et ± 16 g, d'un gyroscope haute fréquence ± 4000 dps et d'un altimètre. Cet article résume les résultats d'expériences en laboratoire pour déterminer les coefficients de restitution de sable et roche. Les caractéristiques des blocs de test montrent que la restitution d'énergie peut varier considérablement pour différentes formes de blocs et surfaces d'impact. Cette étude paramétrique visait à développer une méthodologie préliminaire pour évaluer et améliorer les paramètres d'entrée dans la modélisation informatique des chutes de blocs et aider avec les méthodes d'atténuation. Les trajectoires obtenues à partir des expériences sur le terrain des chutes de blocs ont également été comparées à des modèles de chutes de blocs 2D pour évaluer les coefficients obtenus expérimentalement.

KEYWORDS: Rockfall, Smart Rock, Coefficient of restitution, Rockfall modeling.

1 INTRODUCTION

Rockfall events are an increasingly relevant topic as climatic changes lead to further erosion of slopes, cliffs, and rocky terrains. Weathering processes dislodge portions of slopes, which lead to rockfall and pose a safety hazard to motorists, infrastructure, and buildings nearby. Rockfall trajectories are typically simulated through computational modeling to assist in the design of protective structures. However, the uncertainty related to rockfall behavior and model input parameters is still significantly high.

Rock bouncing motion occurs when falling blocks impact the rock slope or other surfaces (sand, grass, gravel, asphalt). Although the rebound behavior depends on block characteristics that vary for a single site (shape, weight, and size) and the impact surface, the rebound behavior is mathematically governed by one or two coefficients, designated as coefficients of restitution (COR). There are currently multiple physics definitions and interpretations in the literature (Table 1), and the lack of consensus on the most accurate analysis approach illustrates the existing gap to achieve the necessary understanding of rockfall (Chau et al., 2002; Heidenreich, 2004; Turner & Duffy, 2012).

Several authors conducted experimental studies to determine COR values for typical surfaces near rock cuts, including the rock face itself, and better understand rockfall behavior in general. However, restitution coefficients depend on several parameters, which vary according to the block characteristics and impact conditions. Previous assessments in both the laboratory and the field mostly considered impacts of individual blocks. Table 2 presents typical ranges of coefficients of restitution observed for different impact surfaces following the velocity-based definitions for normal and tangential restitution. It can be observed how the energy restitution varies depending on material and test conditions.

The present-day protective structure design is based on velocity and kinetic energy estimates, which typically disregard or inaccurately predict essential aspects of rockfall modeling such as rotational energy and rock rebound (Turner & Duffy, 2012). In addition to overly conservative simulation models, current methods of rockfall analysis typically include field/laboratory measurements, high-frame video recording systems, and detailed event back-analyses. However, these techniques often do not provide detailed information about rock-surface interaction and translational and rotational rock kinematics (Caviezel & Gerber, 2018). To address this issue, researchers have started to instrument test rocks with high-rate sampling acceleration and rotational velocity sensors in field rockfall experiments (Caviezel et al., 2018; Disenhof, 2018).

Research conducted at the University of New Hampshire (Durham, NH, USA) over the last decade developed and improved four generations of Smart Rock (SR) sensors, capable of instrumenting field and laboratory rockfall experiments from the perspective of the falling rock (Harding, 2011; Gullison, 2013; Harding et al., 2014; Apostolov, 2016; Apostolov & Benoît, 2017; Disenhof, 2018).

In this paper, a preliminary instrumented small-scale experimental campaign was conducted to evaluate coefficients of restitution on granular material and rock. The obtained COR values were used as model input parameters in two-dimensional rockfall simulations and compared to trajectories obtained from default coefficients. Both models were compared to trajectories measured in field experiments conducted at a 15 m tall, high-hazard rock cut in Warner, New Hampshire, USA.

Table 1. Velocity- and energy-based COR definitions, retrieved from Turner and Duffy (2012).

	Equation	Terms
Velocities	$COR_{VN} = \frac{v_{RN}}{v_{IN}}$ (1)	COR_{VN} = normal COR v_{RN} = normal translational velocity immediately after impact v_{IN} = normal translational velocity immediately before impact
	$COR_{VN} = \sqrt{\frac{h_{N+1}}{h_N}}$ (2) (free fall at 90º)	h_{N+1} = height of the current bounce h_N = height of the last bounce or drop height for the first bounce
Energies	$COR_E = \frac{0.5mv_{N+1}^2}{0.5mv_N^2}$ (3)	COR_E = energy-based COR m = mass of the block v_{N+1} = scalar velocity after impact v_N = scalar velocity before impact
	$COR_{TE} = \frac{0.5[m(v_R^2)+I\omega_R^2]}{0.5[m(v_I^2)+I\omega_I^2]}$ (4)	COR_{TE} = total energy COR m = mass of the block v_R =scalar velocity after impact v_I = scalar velocity before impact I = moment of inertia of block ω_R = angular velocity after impact ω_I = angular vel. before impact

Table 2. Typical ranges of COR_{VN} used in rockfall modeling.

Source	*Rock*	*Soil*	*Rock talus*
Default (Rocscience)	0.35	0.30	0.32
Literature	0.12 to 0.88 Peng (2000) Asteriou et al. (2012)	0.10 to 0.32 Peng (2000) Pfeiffer and Bowen (1989)*	0.07 to 0.45 Peng (2000) Heierli (1985)*

* Cited by Heidenreich (2004)

2 SMART ROCK

Smart Rock sensors have been used extensively at the University of New Hampshire to characterize rock movement over time. The latest fourth-generation Smart Rocks consist of 3D printed capsules 50.8 mm in length and 25.4 mm in diameter (Figure 1), equipped with a ±400 g and a ±16 g 3-axis accelerometer, a ±4000 dps high-rate gyroscope, an altimeter, and a temperature sensor. The Smart Rock records acceleration, rotational velocity, altitude, and temperature data at a sampling frequency of 100 Hz or 500 Hz (altimeter not enabled) while embedded at the center of gravity of test blocks. A plexiglass window allows the operator to verify that the sensor is turned on and recording data, which is automatically saved to a micro-SD card as a .csv file.

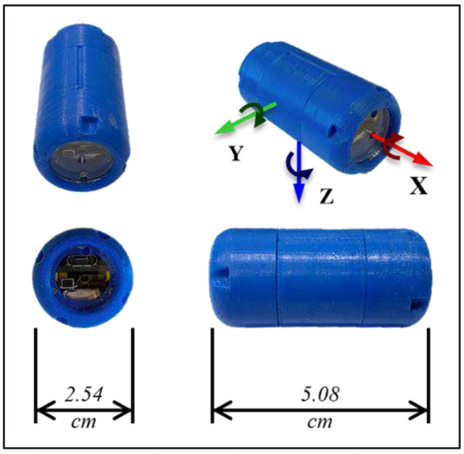

Figure 1. Fourth-generation Smart Rock sensor.

The dual accelerometers allow the SR to capture the full range of accelerations the test rock may experience during a rockfall. While the ±400 g accelerometer captures more significant magnitude accelerations produced by higher impacts from a fall or a bounce, the ±16 g accelerometer captures smaller magnitude accelerations not gathered from the high-g accelerometer since accelerations within ±2 g are typically obscured by noise. The ±16 g accelerometer was limited purposely to ±8 g to decrease noise in the acceleration signal; this can be changed to ±2 g, ±4 g, or ±16 g, as desired. The low-g accelerometer presents a significant advantage in evaluating the rock behavior as it allows users to identify whether the rock is in free fall or at-rest.

3 SMALL-SCALE DROP TESTS

3.1 *Methodology*

Energy restitution experiments were carried out in a test pit in the UNH Geotechnical Laboratory. A Kinsman Granodiorite test rock from Warner/NH was initially cut into a cubic block with approximately 8 cm sides. Next, the block was drilled in its center of gravity with a 2.54 cm core bit and painted for video analysis. In a second round of tests, the block edges were cut with a custom 3D printed fixture aid, and the resulting polyhedron was similar to a cuboctahedron. The results were used to evaluate how rock kinematics during and after impact were affected by shape alteration. The properties of the released block for each shape are presented in Table 3.

Table 3. Properties of the test blocks used for the laboratory experiments.

Block	*Weight (g)*	*Density (kg/m³)*	*Moments of inertia (kg.m²)*		
			I_{XX}	I_{YY}	I_{ZZ}
Cube	1095	2870	0.0010	0.0011	0.0012
Cuboctahedron	790	2870	0.0005	0.0006	0.0006

The first tests were conducted on a 50 cm layer of fine sand (Table 4), compacted using a jackhammer tamper plate until obtaining a medium dense surface with relative density between 50% and 60%. Compaction control was performed with a dynamic cone penetrometer, and the in-place dynamic deflection modulus (Evd) was estimated with a lightweight deflectometer (model Zorn ZFG 2000, 10 kg mass, 200 mm base plate).

To perform each test, the sensor was initially activated, causing it to self-calibrate then start recording. Next, the SR was placed inside the drilled rock holes, and an expandable rubber plug with a through-hole screw was used to hold the SR securely inside the block. Finally, the test block was consistently dropped from a drop device (Figure 2a). This device has a trap door mechanism (Figure 2b), in which the block is placed between two rectangular doors, opened when a lever is pulled (Figure 2c). This mechanism allows the test block to fall with no rotation motion. The box height can be freely adjusted within the frame, allowing tests to be conducted consistently with different drop heights. For these tests, the rock dropper was set up at a constant drop height of 2.2 m.

Table 4. Index properties of the fine sand used as impact surface.

Grain size	D_{10}	D_{30}	D_{60}
	0.10 mm	0.16 mm	0.30 mm
	C_u	C_c	*USCS classification*
	3.0	0.9	Poorly graded sand (SP)
Soil strength	*Friction angle (ϕ')*		E_{vd}
	35º		4.5 MPa

Each experiment was recorded with a frontal (iPhone 11, 240 fps, Figure 2a) and an upper camera (GoPro Hero 4, 120 fps, Figure

2a), whose field of view is presented in Figure 2d. This camera setup allowed recording rock motion about three directions during impact and calculating accurate kinetic energy estimates when matched with the rotation sensor data. The velocities of the released block were estimated through Tracker 5.1.5 software, used to track the center of gravity of the falling block in each video frame. The video recording scale was calibrated with the aid of prism poles.

Ten drop tests from a 90º release angle on the flat, granular material surface were conducted for each test block. After each test, the maximum embedment depth was measured with a caliper, and the test surface was leveled and prepared for the subsequent trial.

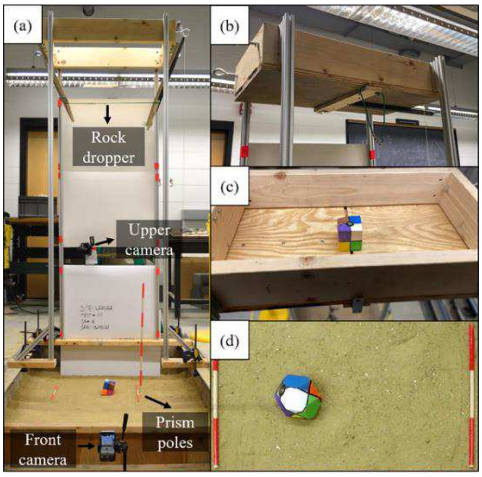

Figure 2. (a) Laboratory test setup, (b) rock dropper, (c) block position before testing, and (d) plane view from the upper camera. The reference sections in the prism poles are 10 cm long.

In a third stage, 90º drop tests were performed on a 60 cm x 30 cm x 15 cm Kinsman Granodiorite also retrieved at the Warner site, embedded in plaster for a precise adjustment of the surface angle at 0º. In order to conduct the experiments from the same drop height of 2.2 m, approximately 15 cm of sand was removed from the test pit, and the granodiorite block embedded in plaster was placed on compacted sand. An LWD modulus of Evd = 80 MPa was measured for the rock on this experimental setup.

The drop tests using the cuboctahedron block on rock were evaluated following the same procedure described for the granular material assessments. Only two trials could be completed, as the test block split in tension during the third test.

The tests were instrumented with Smart Rocks at a sampling frequency of 500 Hz, and the altimeter was disabled due to its significant data noise at high frequencies. The drop took approximately 0.7 seconds from release to hitting the soil or rock surface at each test. It was verified by both Smart Rock and video measurements that the test block did not rotate during free fall in all trials. Each test signal could be easily identified through a sharp peak in acceleration upon impact, which was used to match the sensor and video data to the same time intervals.

The estimated bounce heights, velocities, and kinetic energies from these experiments were used to calculate coefficients of restitution, as displayed in Table 1. Sections 3.2 and 3.3 describe observations from both test sets on sand and rock, and the obtained results are discussed in section 3.4.

3.2 *Tests on sand*

The different responses of both shapes on the granular material surface yielded significantly distinct coefficients of restitution, demonstrating the variability of restitution parameters cited in the literature for different test conditions in rockfalls.

3.2.1 *Cubic block*

All tests described a perfectly vertical (90º angle) trajectory prior to impact. Small bounce heights followed all impacts and a small horizontal displacement before a complete stop. Both front and upper views of a sample test with the cubic block on the sand are shown in Figure 3.

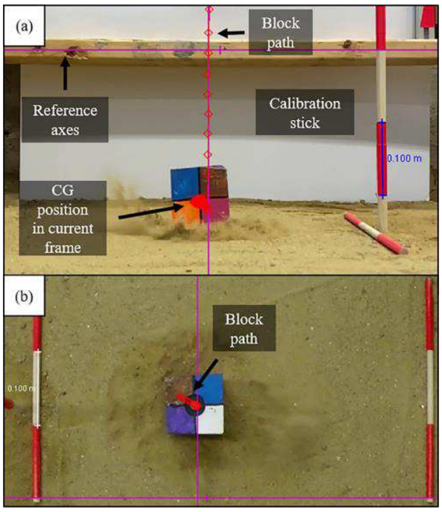

Figure 3. Drop test on sand (cube): (a) frontal and (b) upper camera.

A bounce height of approximately 17 mm was observed for this test. An impact velocity of 7.1 m/s was estimated through video, with vertical and horizontal rebound velocities of 0.7 and 0.3 m/s, respectively, resulting in a scalar velocity of 0.75 m/s after impact. In addition, the resultant rotational velocity after impact, measured with the SR, was equal to 255 dps. Using the velocity definition of COR_VN, the value of 0.10 was obtained. This result is compatible with the alternative definition of COR_VN, specified from the ratio of bounce heights (measured bounce/drop height), equal to 0.09. In contrast, both energy-based coefficients (COR_E and COR_TE) were equal to 0.011. This test yielded total kinetic energies before and after impact equal to 27.6 and 0.3 J, representing a significant energy loss after free fall. Slight rotation was developed due to the angle of impact, and the rotational KE only represented 4% of the translational KE immediately after impact. Finally, the maximum embedment measured was equal to 12.5 mm.

3.2.1 *Cuboctahedron*

Higher block embedment was measured in all trials with the cuboctahedron and equal to approximately double the ground deformations measured in the previous tests. In addition, the lower energy restitution observed in the video recordings caused the test block to tilt diagonally upon impact with increasing depth instead of experiencing small bounces noted for the cubic blocks.

The higher embedment depth and loss of energy also caused a higher volume of granular material to be disturbed in the surroundings of the test blocks, turning video tracking after impact into a difficult test to estimate the CG position after impact. The block rotation with the tilting behavior was also an obstacle during video tracking. During all experiments, bouncing behavior was not visually observed.

The horizontal displacement of the test block was more significant than before cutting the edges of the cubic block, as shown in Figure 4. This test yielded total kinetic energies before and after impact equal to 19.8 and 0.13 J, representing a significant loss of kinetic energy after free fall. The higher rotation developed due to the block shape led to a ratio between rotational and translational energies equal to 24%, a significantly higher contribution than the test presented for the cubic block, even though the total energy restitution was smaller. The maximum embedment measured after the test was equal to 23.4 mm. For this experimental trial, the restitution coefficients COR_VN, COR_E, and COR_TE were equal to 0.014, 0.005, and 0.006, respectively.

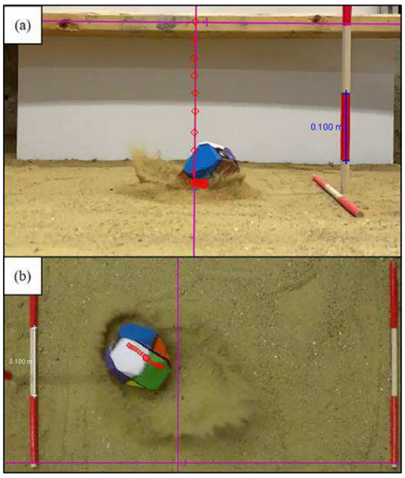

Figure 4. Drop test on sand (cuboctahedron): (a) frontal and (b) upper camera.

3.3 *Tests on rock*

Finally, the tests on the rock surface described significantly distinct trajectories and energy restitution compared to the tests on sand. Bouncing behavior could be identified in the video, and rock displacement occurred in all three directions (vertical, parallel to the frontal camera, and towards the frontal camera). Figure 5a shows the trajectory described by the test block in the first trial on rock. Compared to the tests on granular material, a clear bounce can be visualized, and significant energy restitution was estimated compared to the previous trials. The direction of the bounce was expected due to a small slope at the landing point. Figure 5b displays the plan view of the drop test. The lateral dispersion perpendicular to the front camera was nearly zero.

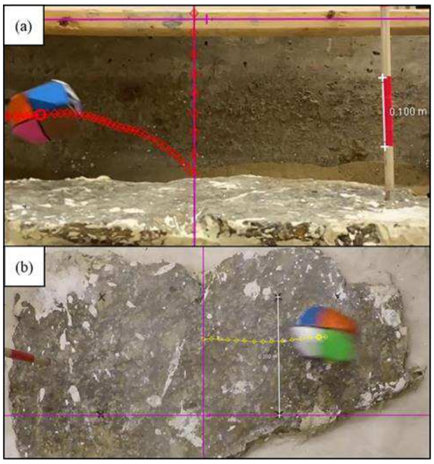

Figure 5. Drop test on rock: (a) frontal and (b) upper camera.

The rotational rate described by the test block during the first bounce is equal to the rotational velocity of the cubic block after the impact on sand (500 dps). An impact velocity of 7.2 m/s was estimated through video, with vertical and horizontal rebounds velocity of 1.5 and 2 m/s, respectively. This test yielded total kinetic energies before and after impact equal to 20.2 and 2.5 J, representing a loss of 88% of the kinetic energy after free fall. Slight rotation was developed due to the angle of impact, and the rotational KE only represented 1% of the translational KE immediately after impact.

During the rebound behavior, a bounce height of approximately 88 mm was measured. Using the velocity definition of COR_VN, a value of 0.21 was obtained for this test. This result is compatible with the alternative definition of COR_VN, specified from the ratio of bounce heights (measured bounce/drop height), which was equal to 0.20 for the same test. Both kinetic energy-based COR definitions (COR_E and COR_TE) were equal to 0.12. The second test on rock deviated from the plane parallel to the front camera and had a maximum bounce height of 170 mm. Despite the trajectory variability, both tests on rock had similar coefficients of restitution.

3.4 *Results and discussion*

Table 5 presents a summary of the Smart Rock data for all experiments. The measured three-axis acceleration and rotation data could be used to calculate resultant acceleration and rotational velocity magnitudes. Resultant accelerations were used to estimate impact forces experienced by the test block, if multiplied by the block weight. Smaller mass objects with less contact area are subject to higher accelerations upon impact on a stiffer surface (Leonhardt, 2001). Thus, both trials on rock experienced higher acceleration than the sand tests and exceeded the measuring limits of the high-g accelerometer.

Table 6 presents a summary of the block kinematics before and after impact. For all tests, the rotational kinetic energy contribution of all tests was minimal due to the 90º impact angle. Higher block rotation and tangential velocities are expected on inclined impact surfaces and/or stiffer materials such as rock.

The normal coefficients of restitution obtained from the trials with the cubic block are in close agreement with previous assessments on granular material performed by Peng (2000) (COR_VN between 0.10 and 0.12 for soil), and in the lower limit of the COR_VN range between 0.10 – 0.20, specified by Jones et al. (2000, cited by Heidenreich, 2004), for soft soil slopes. In addition, the estimated normal coefficients of restitution are significantly lower than default coefficients used in two-dimensional modeling, published by Hoek (1987, cited by Heidenreich 2004) and Pfeiffer and Bowen (1989, cited by Heidenreich, 2004), equal to approximately 0.30.

The higher energy dissipation observed with the cuboctahedron tests yielded lower COR values and increased the variability in results. The obtained range of velocity- and energy-based COR values are comparable to results obtained at the small-scale parametric experimental campaign conducted by Heidenreich (2004). Peng (2000) performed tests with spherical blocks released on coarse sand, which yielded normal coefficients of restitution equal to zero. However, assuming zero restitution on sand slopes potentially underestimates rockfall trajectories and can increase the risk of hazards to the public.

Finally, the tests on rock presented a significantly distinct behavior compared to the sand tests. As observed by authors such as Pfeiffer and Bowen (1989, cited by Heidenreich, 2004), Fornaro et al. (1990, cited by Heidenreich, 2004), and Chau et al. (2002), impact surfaces with higher Young's modulus will also increase energy restitution in both normal and tangential directions. Although the described trajectories were different while bouncing, the test blocks presented similar velocity- and energy-based coefficients of restitution. The COR values from both tests on rocks are

Table 5. Smart Rock data summary.

Material	*Average block embedment (mm)*	*Smart Rock resultant data*			*Maximum impact force (kN)*
		Max. acceleration (g)	*Max. rotational velocity (dps)*	*Avg. rot. vel. (dps)*	
Sand (cube)	12.1 ± 1.9	324 ± 85	711 ± 275	38 ± 15	3.5 ± 0.9
Sand (cuboct.)	24.8 ± 1.1	185 ± 33	636 ± 119	73 ± 14	1.5 ± 0.3
Rock* (cuboct.)	-	489**	2894	378	3.8

* Based on 2 experimental trials (block fragmentation). **High-g acceleration measuring range was exceeded upon impact.

Table 6. COR results for the drop tests on sand using the cubic block.

Material	*Average coefficients of restitution*			
	COR_{VN} (bounce heights)	*COR_{VN}*	*COR_{E}*	*COR_{TE}*
Sand (cube)	0.08 ± 0.01	0.08 ± 0.01	0.008 ± 0.002	0.008 ± 0.002
Sand (cuboct.)	-	0.03 ± 0.02	0.003 ± 0.001	0.004 ± 0.002
Rock (cuboct.)	0.24	0.21	0.11	0.11

compatible with field and laboratory results from Urciuoli (1988, cited by Heidenreich, 2004), Peng (2000), Ushiro et al. (2000, cited by Heidenreich, 2004), and Asteriou et al. (2012). However, most of the energy assessments published in the literature present higher restitution values, including default coefficients used in modeling software.

The video and sensor measurements demonstrated that the cubic block, which had a larger surface contact area during impact, presented a distinct behavior from the cuboctahedron. Table 7 displays the differences in behavior observed in both samples under identical release and impact surface conditions. It was identified that the block penetration in the sand governs the rebound and energy restitution behavior. Higher embedment depths (ground deformation) implied higher rotation and a rolling behavior instead of block bouncing. Past rebound assessments on plaster performed by Chau, Wu et al. (1999), cited by Heidenreich (2004), have also shown higher normal coefficients of restitution for cubic blocks than spherical blocks.

Table 7. General observations of rockfall behavior during the experimental campaign.

Parameter	*Flat contact area*	*"Rounded" contact area*
Acceleration	↑ Increases	↓ Decreases
Block rotation	↓ Decreases	↑ Increases
Lateral dispersion	↓ Decreases	↑ Increases
Block embedment	↓ Decreases	↑ Increases
Block rebound	↑ Increases	↓ Decreases

The change in behavior with the alteration of the shape of the test follows observations from Heidenreich (2004), who meticulously studied block impacts on soft ground. They defend that the rebound behavior is controlled by block penetration, sliding, and rotation, as impacts on soft ground typically do not have enough KE to deform the released blocks plastically. Heidenreich also states that vertical impacts on soft horizontal ground, even if compacted, produce very small to no rebound in the vertical direction. However, more significant rebound behavior can be observed upon impact at inclined conditions.

The investigation conducted by Heidenreich (2004) demonstrated a high complexity associated with block bouncing on soft ground, which produces a significant variability in restitution coefficients with different surface conditions. Heidenreich reiterated that default coefficients of restitution published in the literature are prone to inaccurate predictions if applied to another site and/or test conditions. Therefore, it is challenging to select representative parameters for trajectory predications upon impacts on soil. In this context, Heidenreich recommends the verification of rockfall models with field trials for protective assessments of areas at risk.

4 ROCKFALL MODELING

The obtained COR_VN values were evaluated in a digital rockfall model of a 15 m road cut in Warner/NH, where eight field rockfall experiments were performed with local rocks for model comparisons (Souza, 2021). According to the Rockfall Hazard Rating System, the slope is classified as a high hazard being 3.5 to 5 meters away from the road. The catchment ditch is flat and composed of granular soil.

These simulations were performed using RocFall software by Rocscience, which can calculate bounce heights, energies, and velocities for 2D trajectories. The model results obtained from the laboratory coefficients were compared with models using default coefficients (Table 8). The software imported the slope cross-sections as coordinates obtained from 3D surface models generated by photogrammetry by the New Hampshire Department of Transportation. Representative cross-sections from each field test were extracted from the 3D slope model.

Table 8. Coefficients of restitution (respectively): normal coefficient of restitution, dynamic coefficient of friction, and rolling coefficient of friction. Source: Rocscience, Coefficient of Restitution table.

	Description	COR_{VN}	μ	μ_r
Default	🟩 Slope: bedrock outcrops	0.35±0.04	0.55±0.04	0.15±0.04
	🟨 Ditch: soft soil, some vegetation	0.30±0.04	0.55±0.04	0.30±0.02
	⬜ Road: asphalt	0.40±0.04	0.55±0.04	0.10±0.01
Lab.	🟩 Slope: bedrock outcrops	0.21±0.04	0.55±0.04	0.15±0.04
	🟨 Ditch: soft soil, some vegetation	0.08±0.02	0.55±0.04	0.30±0.02

Rigid body analyses were performed for each test rock, whose mass, shape, and density were imported for each assessment. For more straightforward data processing in 2D, the geometry of each rock was simplified, and all rocks were simulated in two directions to account for rotation about multiple axes. Each rock cross-section was simulated 50 times, from the same approximate drop locations of the field tests.

Figure 6 presents the modeled rock shapes and trajectories for an 18 kg block. The red trajectories represent the cross-section with rotation about the axis of lowest inertia, while the green trajectories represent the cross-section that rotates about the axis of highest inertia. The black trajectory was approximated from the field experiment, and the block had a ground impact energy that was wholly absorbed (zero bounce height).

Compared to the field tests with the same rocks and slope cross-sections, the modeled rockfall motion type (free fall, rolling, bouncing) before ground impact typically agreed with the field observations. However, the quantitative data (bounce heights, runout, and rotational velocities) were often overestimated, leading to overly conservative ditch geometry and protective structures. Although the laboratory-based coefficients estimated smaller bounce heights more compatible with the field behavior, the rotational motion was not significantly decreased after the first impacts with the ground as observed in the field.

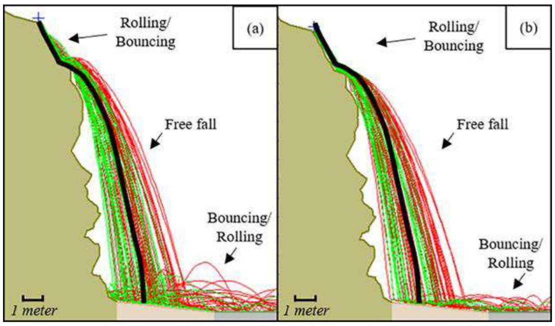

Figure 6. Modeled rockfall trajectories using (a) default and (b) laboratory coefficients. The trajectory in black represents the field test.

Therefore, these early results suggest that the current predictive methods used in this paper were not fully compatible with the recorded data and measured runouts from the full-scale experiments. These recent models typically assume restitution and friction parameters, resulting in an unsafe or overly conservative design. There is an increasing need to estimate coefficients of restitution capable of realistically predicting the dispersion of falling rocks in typical surfaces, and the Smart Rock can be considered a promising tool for more accurate assessments and consequent hazard mitigation.

5 CONCLUSION AND FUTURE PERSPECTIVES

There is an increasing need to estimate coefficients of restitution capable of realistically predicting the dispersion of falling rocks in typical surfaces, and the Smart Rock can be considered a promising tool for accurate energy assessments and consequent hazard mitigation. SRs have been demonstrated as simple and reliable instruments capable of accurately measuring rockfall motion. The obtained acceleration and rotational velocity outputs can be used to validate and improve rockfall computational models and help with mitigation methods.

The experimental laboratory setup discussed in this paper was successful in developing a preliminary methodology for energy assessments of falling blocks using a Smart Rock sensor. The three series of tests confirmed observations from previous authors that the rebound behavior of falling blocks depends on a wide variety of simultaneous factors. The ground characteristics (material, inclination, conditions), block properties (weight, geometry), and fall kinematics (impact velocity, impact angle, block rotation) exert a crucial role in the developed bounce heights and runout distances. This way, distinct responses can be produced for the same block if the test conditions are altered.

Coefficients of restitution in rockfall modeling need to account for several impact conditions and provide the most probable responses for subsequent sizing of protective structures. Preliminary model comparisons have suggested that laboratory-based model input parameters reproduce more realistic rockfall trajectories, including bounce heights and runout distances, compared to default coefficients. The model results indicate that further investigation is still required to assess the overestimated rotation and runout data. The designed laboratory methodology has a high potential to evaluate bouncing behavior through instrumented tests on different impact surfaces at a range of surface inclinations and drop heights.

Extensive field and laboratory experiments are being conducted at the University of New Hampshire to gather data on several rock slopes of different geometries, with variable sizes and shapes of test rocks. In addition, future small- and medium-scale laboratory testing will be used to evaluate rock rebound under different releasing block and impact surface conditions. Several rockfall influencing parameters, including block and impact surface characteristics, and falling block kinematics, will be assessed. The objective is to use the experimental data to determine modeling aspects that require better qualification.

Therefore, given that most past coefficient of restitution assessments published in the literature were performed on a small scale (database outlined in Souza, 2021), Smart Rocks can efficiently evaluate and directly compare rock rebound in small- and medium-scale laboratory experiments to large-scale field instrumented tests. Results from these comparisons can be used to evaluate the accuracy of 2D and 3D rockfall models using different input parameters.

6 ACKNOWLEDGEMENTS

The authors would like to thank the New Hampshire Department of Transportation Bureau of Materials and Research, especially Neil Olson and Krystle Pelham, for all the support to conduct this experimental research. Acknowledgments also to Artur Apostolov for developing the Smart Rocks used in this research.

7 REFERENCES

Apostolov, A. & Benoît, J. 2017. Motion tracking “Smart Rock” device for the study of landslide and debris flows mechanisms. *North American Symposium on Landslides*, Roanoke, VA, USA, 889-900.

Apostolov, A. 2016. Development and testing of motion tracking “Smart Rock” devices for geotechnical applications. (Master’s thesis). University of New Hampshire, Durham, NH.

Asteriou, P., Saroglou, H., & Tsiambaos, G. 2012. Geotechnical and kinematic parameters affecting the coefficients of restitution for rock fall analysis. *International Journal of Rock Mechanics and Mining Sciences*, 54, 103-113.

Caviezel, A., & Gerber, W. 2018. Brief Communication: Measuring rock decelerations and rotation changes during short-duration ground impacts. *Natural Hazards and Earth System Sciences*, 18(11), 3145-3151.

Caviezel, A., Schaffner, M., Cavigelli, L., Niklaus, P., Bühler, Y., Bartelt, P., & Magno, M. 2018. Design and evaluation of a low-power sensor device for induced rockfall experiments. *ISEE Transactions on Instrumentation and Measurement*. 67(4), 767-779.

Chau, K. T., Wong, R. H. C., & Wu, J. J. 2002. Coefficient of restitution and rotational motions of rockfall impacts. *International Journal of Rock Mechanics and Mining Sciences*, 39(1), 69-77.

Disenhof, C. R. 2018. Investigation of surface models and the use of a Smart Rock for rockfall modeling. (Master’s thesis). University of New Hampshire, Durham, NH.

Gullison, M. 2013. Analysis of Smart Rock data from debris flow experimentation. M.S. thesis, University of New Hampshire, Durham, NH.

Harding, M. J., Fussell, B. K., Gullison, M. A., Benoît, J., & de Alba, P. A. 2014. Design and Testing of a Debris Flow ‘Smart Rock’. *Geotechnical Testing Journal*, 37(5), 769-785.

Harding, M.J. 2011. Design and Development of a Debris Flow Tracking “Smart Rock”. M.S. Thesis, University of New Hampshire, Durham, NH.

Heidenreich, B. 2004. Small- and Half- Scale Experimental Studies of Rockfall Impacts on Sandy Slopes. (Doctoral thesis). École Polytechnique Fédérale de Lausanne, Lausanne, Switzerland.

Leonhardt, P. M. 2001. Acceleration levels of dropped objects. *Endevco Corporation*.

Peng, B. 2000. Rockfall Trajectory Analysis – Parameter Determination and Application (Master’s thesis). University of Canterbury, Christchurch, New Zealand.

Rocscience. “Coefficient of Restitution Table”, [online]. Available at: https://www.rocscience.com/help/rocfall/baggage/rn_rt_table.htm

Souza, B. M. M. 2021. Use of Smart Rocks to improve rock slope design. (Master’s thesis). University of New Hampshire, Durham, NH.

Turner, A.K., & Duffy, J.D. 2012. Evaluation of Rockfall Mechanics. In Turner, A.K. and Schuster, R.L. (Eds). *Rockfall Characterization and Control*, 285-333. Washington, D.C.: Transportation Research Board.